

Zeolitic Imidazolate Framework 67-derived Ce-doped CoP@N-doped Carbon Hollow Polyhedron as High-Performance Anodes for Lithium-Ion Batteries

YanJun Zhai^{1,*}, Shuli Zhou¹, Linlin Guo¹, Xiaole Xin¹, Suyuan Zeng¹, Konggang Qu¹, Nana Wang², Xianxi Zhang^{1,*}

¹ Department of Chemistry and Chemical Engineering, Shandong Key Laboratory of Chemical Energy Storage and Novel Cell Technology, Liaocheng University, Liaocheng, 252059, China;

zhouli1996@126.com (S.Z.); 15506436037@163.com (L.G.); xx115865517198@163.com (X.X.); drzengsy@163.com (S.Z.); qukonggang@lcu.edu.cn (K.Q.)

² Institute for Superconducting and Electronic Materials, University of Wollongong Innovation Campus, Wollongong New South Wales, 2500, Australia; nanaw@uow.edu.au

* Correspondence: zhaiyanjun@lcu.edu.cn (Y.Z.); xxzhang3@126.com (X.Z.)

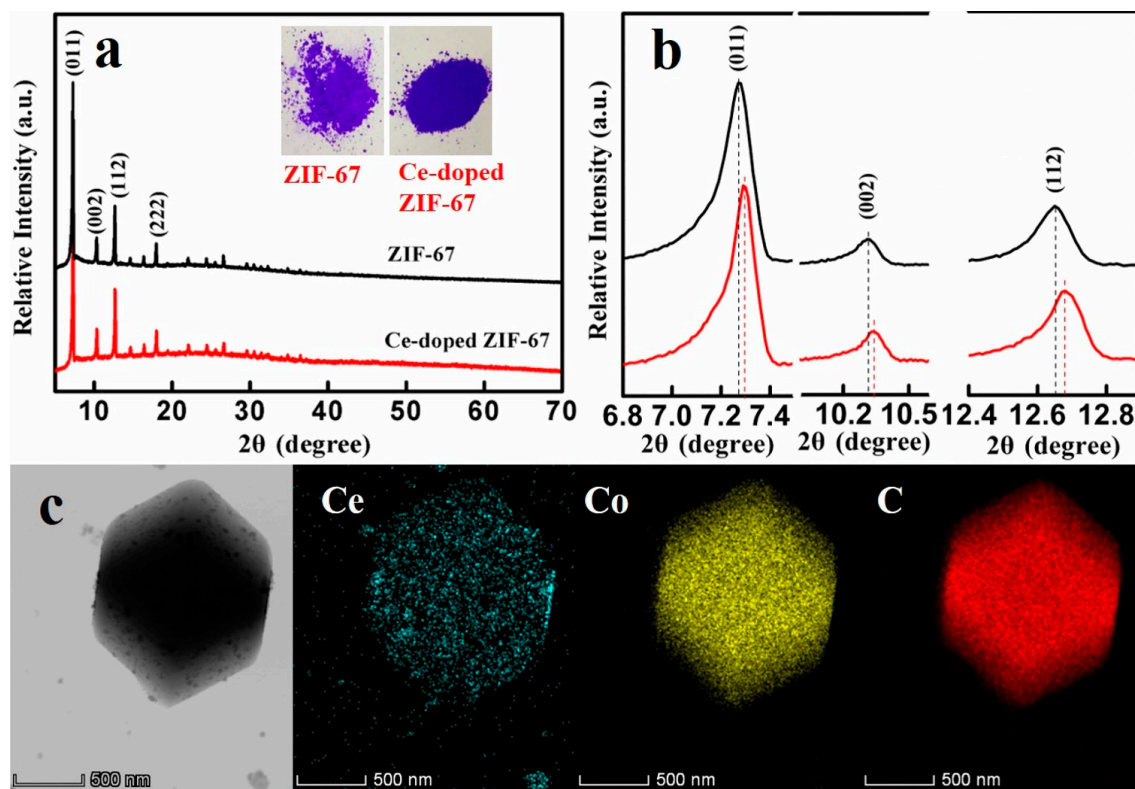


Figure S1. (a) XRD patterns of ZIF-67 and Ce-doped ZIF-67. (b) the magnified region of $2\theta = 16.7\text{--}18.0^\circ$ showing a peak shift. (c) EDX elemental mapping images of Ce, Co and C for Ce-doped ZIF-67.

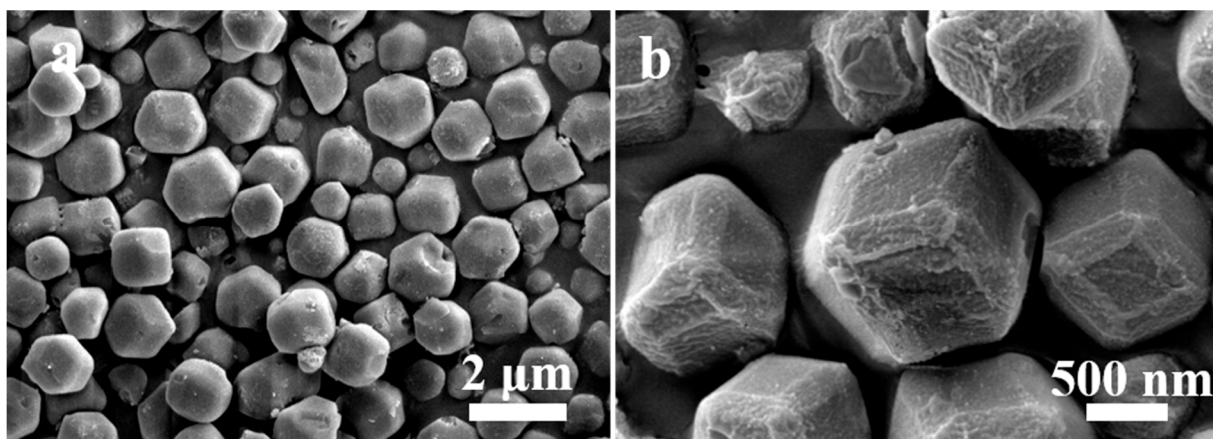


Figure S2. SEM images of Ce-doped ZIF-67.

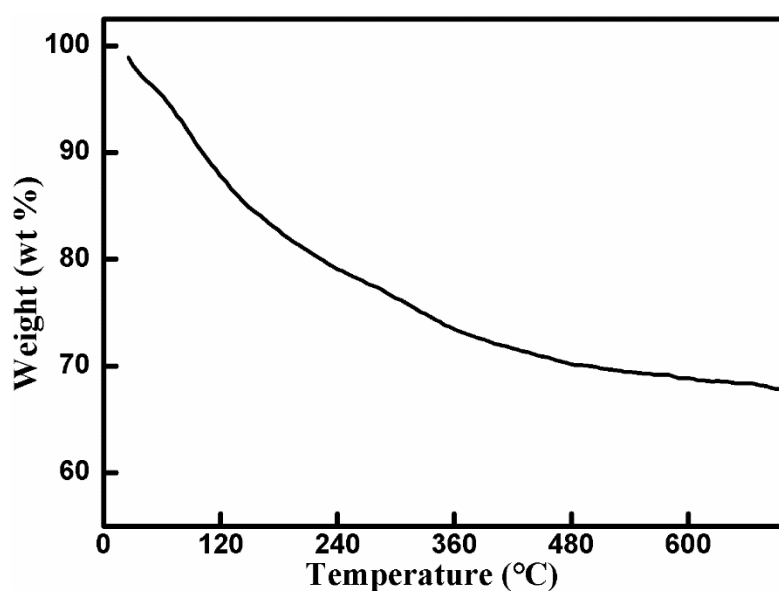


Figure S3. The TGA curves of Ce-doped ZIF-67.

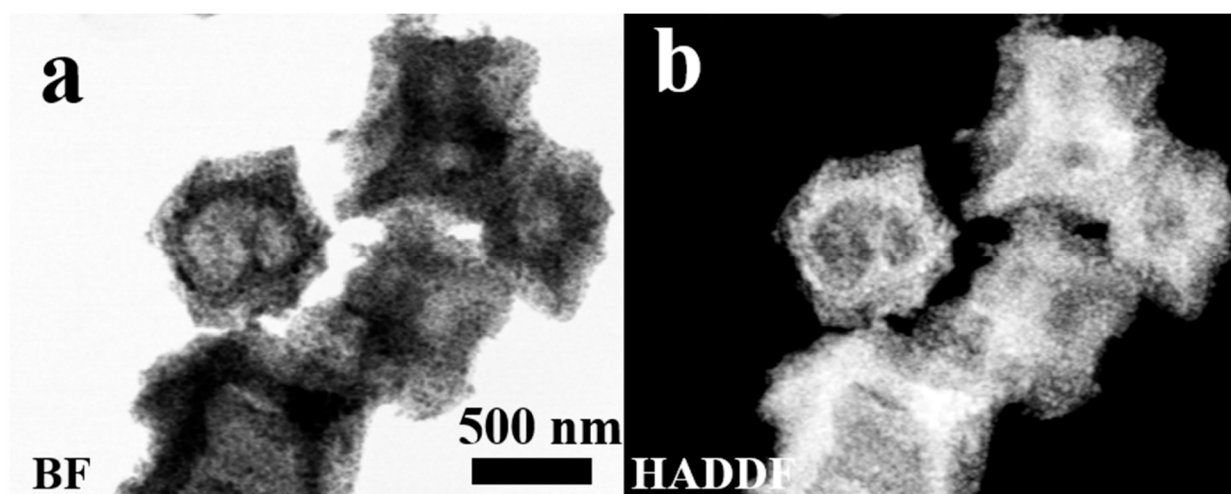


Figure S4. (a) TEM bright field (BF) image, (b) HAADF-STEM image of Ce-doped Co/CN.

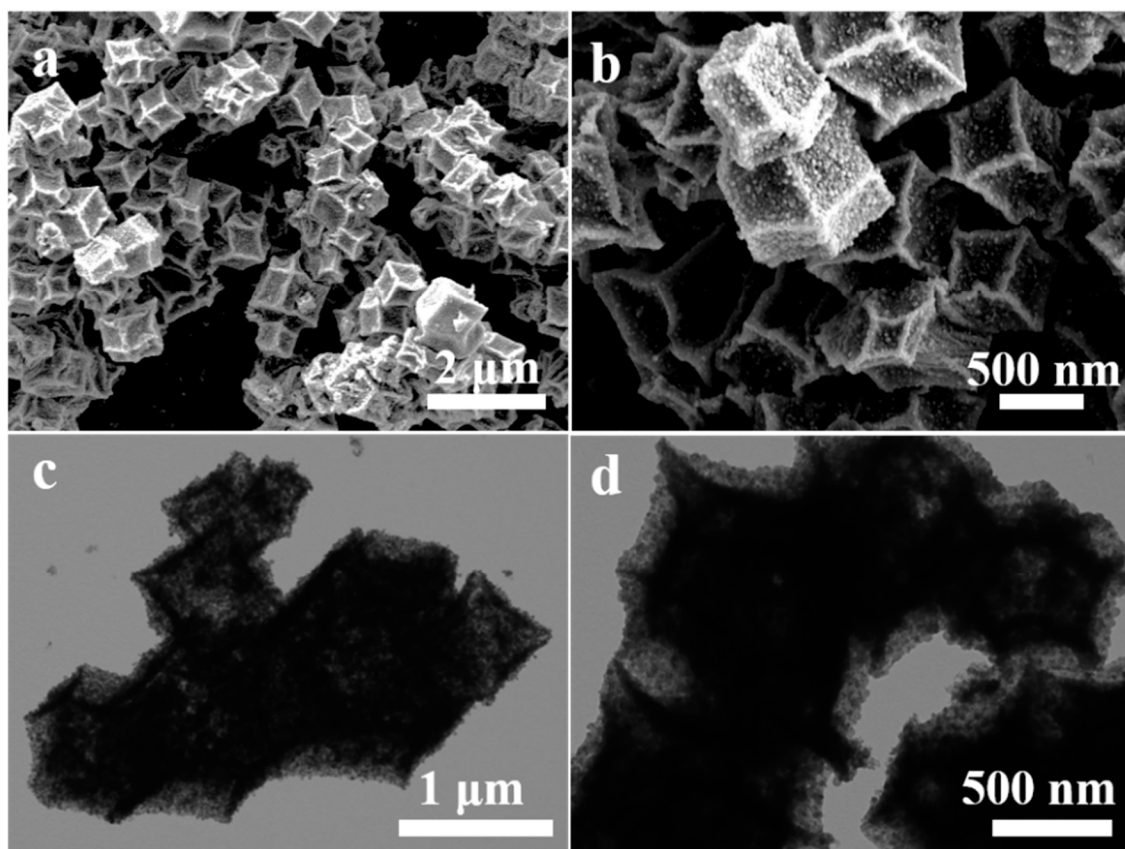


Figure S5. (a, b) SEM images and (c, d) TEM images of CoP.

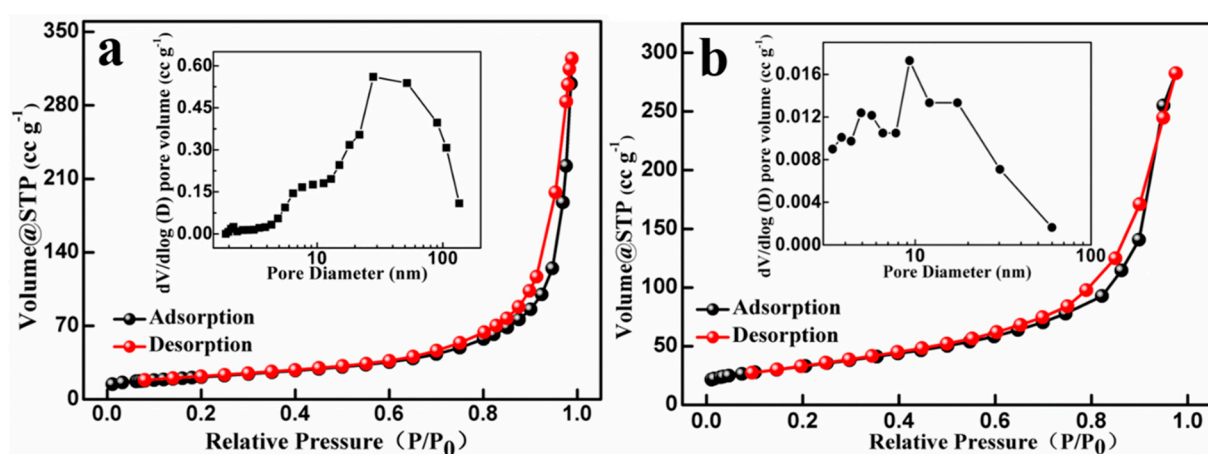


Figure S6. N₂ adsorption/desorption isotherm and the corresponding pore size distributions (inset) of (a) CoP/NC and (b) Ce-doped CoP/NC.

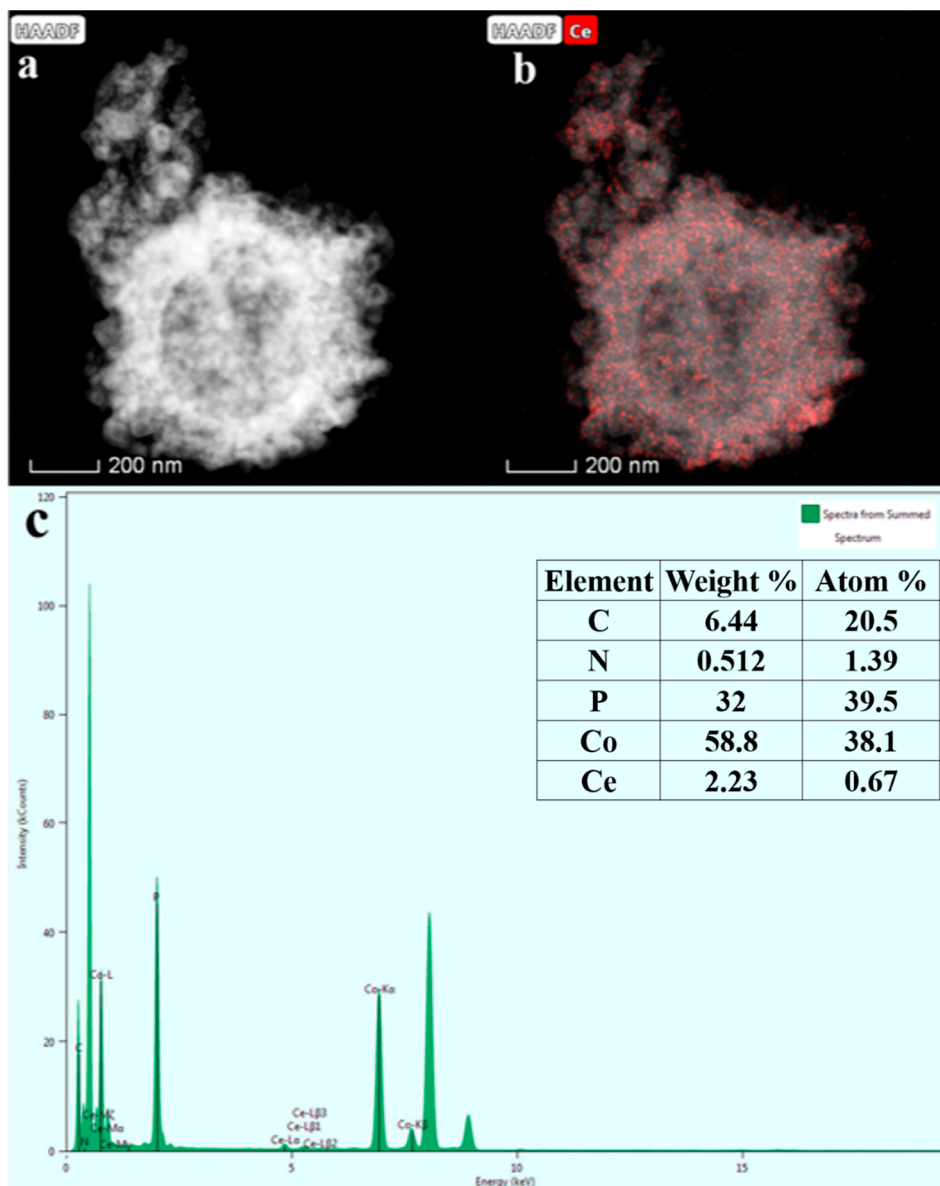


Figure S7. (a, b) HAADF-STEM images and (b) EDX of Ce-doped CoP/NC.

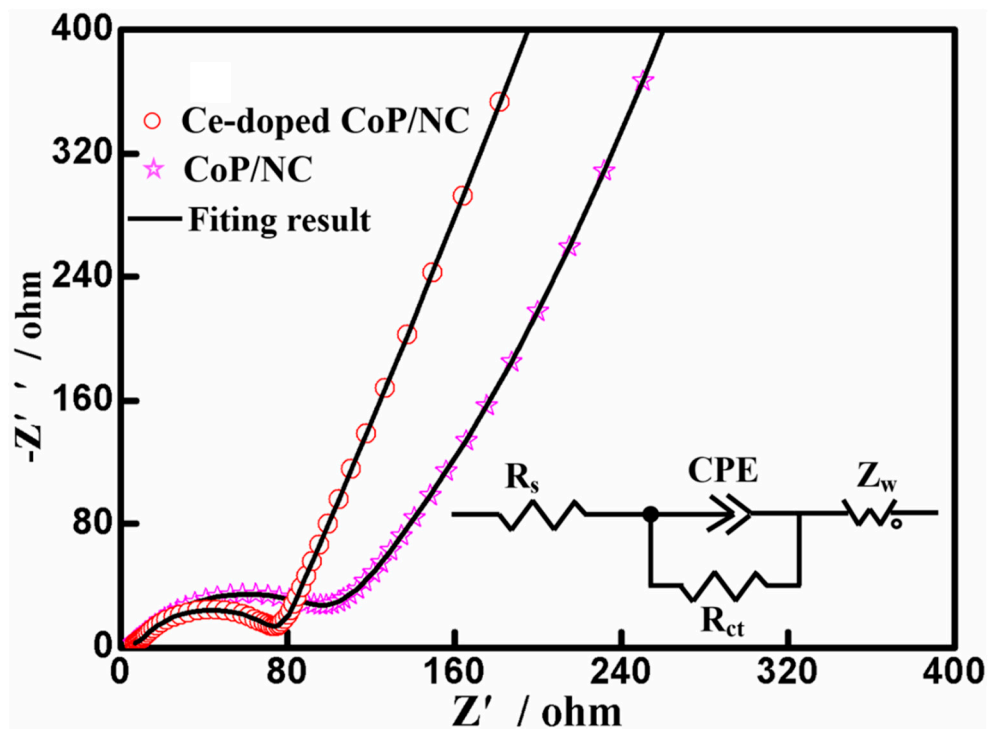


Figure S8. Nyquist plot and equivalent circuit model of Ce-doped CoP@NC and pure CoP@NC electrodes.